

# Generic Contrast Agents

Our portfolio is growing to serve you better. Now you have a *choice*.



[VIEW CATALOG](#)

# AJNR

This information is current as of May 19, 2025.

## **Protuberant Fibro-Osseous Lesion of the Temporal Bone: "Bullough Bump"—Multimodality Imaging Case Series and Literature Review**

N. Shekhrarka, D.R. Shatzkes, K.E. Dean, M.C. Smithgall and G. Moonis

*AJNR Am J Neuroradiol* 2021, 42 (11) 2023-2029

doi: <https://doi.org/10.3174/ajnr.A7298>

<http://www.ajnr.org/content/42/11/2023>

# Protuberant Fibro-Osseous Lesion of the Temporal Bone: “Bullough Bump”—Multimodality Imaging Case Series and Literature Review

 N. Shekhrajka,  D.R. Shatzkes,  K.E. Dean,  M.C. Smithgall, and  G. Moonis

## ABSTRACT

**SUMMARY:** A handful of cases of protuberant fibro-osseous lesions of the temporal bones have been described in the literature to date, with primary focus on the pathologic features. Here we review 3 cases of pathology-proved protuberant fibro-osseous lesions of the temporal bone and include a literature review with a focus on the imaging features. While rare, these lesions have near-pathognomonic imaging features defined by a location at the cortex of the outer table of the temporal bone at the occipitomastoid suture, lack of involvement of the underlying marrow, variable mineralization, and MR signal characteristics atypical of a chondroid lesion. One case in this series was FDG-avid and had occasional mitotic features, possibly reflecting an aggressive variant. Neuroradiologists should be familiar with this benign diagnosis to aid in timely identification and avoid unnecessary additional imaging.

**ABBREVIATIONS:** FD = fibrous dysplasia; PFOLT = protuberant fibro-osseous lesion of the temporal bone

Protuberant fibro-osseous lesion of the temporal bone (PFOLT) was originally described by Selesnick et al,<sup>1</sup> in 1999. They presented 2 unique-but-identical cases of right-sided retroauricular exophytic fibro-osseous lesions in young patients emanating from the outer cortex of the bone near the occipitomastoid suture line. Almost 11 years later, Sia et al<sup>2</sup> reported 2 similar cases in 2010, and they proposed naming the lesion “Bullough lesion/bump” after Professor Peter Bullough, who described the pathologic features in the original case report in 1999. To date, 10 similar cases have been reported in the literature. These lesions have near-pathognomonic imaging features, defined by a location at the outer table cortex of the temporal bone at the occipitomastoid suture, lack of involvement of the underlying marrow, variable mineralization, and MR signal characteristics atypical of a chondroid lesion. The goal of this article is to report a multi-institutional series of this lesion, to discuss the clinical characteristics and unique imaging features of the lesion, and to review the existing cases in the literature.

## Case Series

Institutional review board approval was waived and not required for this retrospective case series. Three cases were identified from 3 different institutions in New York City between 2015 and 2020.

Demographic information was obtained from the electronic medical record, including age, clinical presentation, imaging findings, and histopathologic diagnosis.

**Case 1.** A 39-year-old previously healthy woman presented with a painless mass in the right retroauricular region, which had been slowly growing for the last 5 years. No other contributory history was noted. On physical examination, a nontender mass was palpated in the right retroauricular region without changes in the overlying skin. The mass was hard in consistency, and the overlying skin was freely mobile. No other findings were observed on the clinical examination. Neurologic examination findings were normal, as were hematologic and audiologic parameters.

On skull radiographs, bony thickening of the right retroauricular region with a small exophytic sclerotic/mineralized lesion was noted (Fig 1). Noncontrast CT of the head demonstrated a 3.5 × 1.1 cm, well-defined, broad-based, protuberant calcified mass with ground-glass density in the retroauricular region emanating from the outer cortex of the right temporal bone near the occipitomastoid suture (Fig 2). There was a stalk-like attachment to the outer cortex, with some irregularity of the otherwise intact underlying cortex. No intracranial extension was seen. There was elevation of the overlying scalp. Given the imaging features, the initial differential diagnoses of the lesion included osteoma, osteoblastoma, parosteal osteosarcoma, and periosteal chondrosarcoma. MR imaging

Received March 24, 2021; accepted after revision July 9.

From the Department of Radiology (N.S.), Copenhagen University Hospital, Copenhagen, Denmark; Department of Radiology (D.R.S.), Donald and Barbara Zucker School of Medicine at Hofstra/Northwell, Lenox Hill Hospital, New York, New York; Department of Radiology (K.E.D.), Weill Cornell Medicine, New York, New York; and Department of Pathology (M.C.S.), Anatomic and Clinical Pathology, and Department of Radiology (G.M.), Columbia University Irving Medical Center, New York, New York.

Please address correspondence to Gul Moonis, MD, Department of Radiology, Columbia University Irving Medical Center, 630 W 168th Street, New York, NY 10032; e-mail: gm2640@cumc.columbia.edu; @gmoonis

<http://dx.doi.org/10.3174/ajnr.A7298>

of the brain with and without contrast showed a T1- and T2-hypointense (to muscle), mildly enhancing, broad-based, postauricular lesion emanating from the outer table of the right temporal bone. There was a more pronounced peripheral rim of enhancement noted (Fig 3). There were no signal changes in the underlying bone, nor was there intramedullary or intracranial extension.

The lesion was excised without any postoperative complications. The temporalis muscle was found to be partially adherent to the lesion intraoperatively. A calcified peduncular attachment of the lesion to the outer table was noted, which was resected. Microscopically, there were numerous rounded ossified bodies



**FIG 1.** Case 1. Plain radiographs of the skull show a small, exophytic sclerotic/mineralized lesion with bony thickening of the right retroauricular cortex (white arrow).

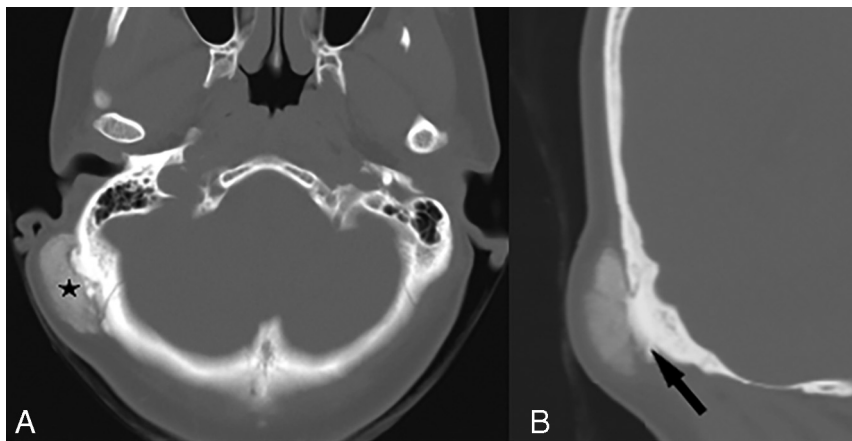


**FIG 2.** Case 1. Axial (A) and coronal (B) noncontrast CT images through the temporal bone show a well-defined, exophytic, protuberant calcified mass with ground-glass density (star) in the retroauricular region, seen emanating from the outer cortex of the right temporal bone near the occipitomastoid suture causing elevation of the overlying scalp without intramedullary or intracranial extension. A broad-based stalk-like attachment to the occipitomastoid suture is noted (arrow).

composed of either woven or lamellar bone within a bland fibrous stroma. Atypia, mitotic activity, or osteoblastic rimming were not identified (Fig 4).

The patient has been followed for 4 years without any evidence of tumor recurrence.

**Case 2.** An 18-year-old man presented with a lump behind the left ear noted by his father 2 years earlier. His father thought that the lump was slowly growing. He had no pain, hearing loss, or history of trauma, and the patient was otherwise healthy. Physical examination showed a  $3 \times 2$  cm left retroauricular bony protuberance over the mastoid area (Fig 5). The remainder of the head and neck examination had normal findings.

He initially underwent noncontrast head CT, which demonstrated a well-margined calcific mass with a sclerotic stalk within the occipitomastoid suture and a larger exophytic component containing punctate areas of osseous and/or calcific density (Fig 6). The initial differential diagnosis included osteochondroma, parosteal osteosarcoma, or chondrosarcoma. MR imaging of the skull base was then performed, demonstrating immediate T1 signal intensity, very low T2 signal intensity (to muscle), and mild heterogeneous contrast enhancement (Fig 7). The low T2 signal intensity was thought incompatible with a chondroid lesion, and the differential was revised to a Bullough lesion versus parosteal osteosarcoma.

A 3-cm fibro-osseous mass with a mushroom-like shape was excised from the outer cortex of the left temporal bone. Histologic analysis revealed rounded or ovoid areas of calcification within a background of bland fibrous stroma, compatible with a Bullough lesion. The postoperative course was uncomplicated, and there has been no recurrence 5 years following resection.

**Case 3.** A 25-year-old woman with a history of retinopathy of prematurity and chronic daily headaches presented with a hard, palpable mass behind her right ear. The patient reported that she initially noticed the mass 2 months prior, and it was slowly growing since that time. The patient denied changes to her existing headaches or other new symptoms. On examination, the lesion was nonmobile, firm, and approximately 2 cm in size.

A head CT at that time identified an irregularly calcified, protuberant mass arising from the outer cortex of the right temporal bone overlying the occipitomastoid suture with no continuity with the medullary cavity (Fig 8). On review of existing head CTs from 2007, 2010, and 2011 (all acquired for headaches), it was noted that the mass had substantially increased in size, now measuring  $2.9 \times 1.5 \times 2.3$  cm, compared with  $0.6 \times 0.3 \times 0.5$  cm in 2007 (Fig 9). In addition to being smaller, the lesion previously appeared solidly calcified in 2007, suggestive of a peripheral

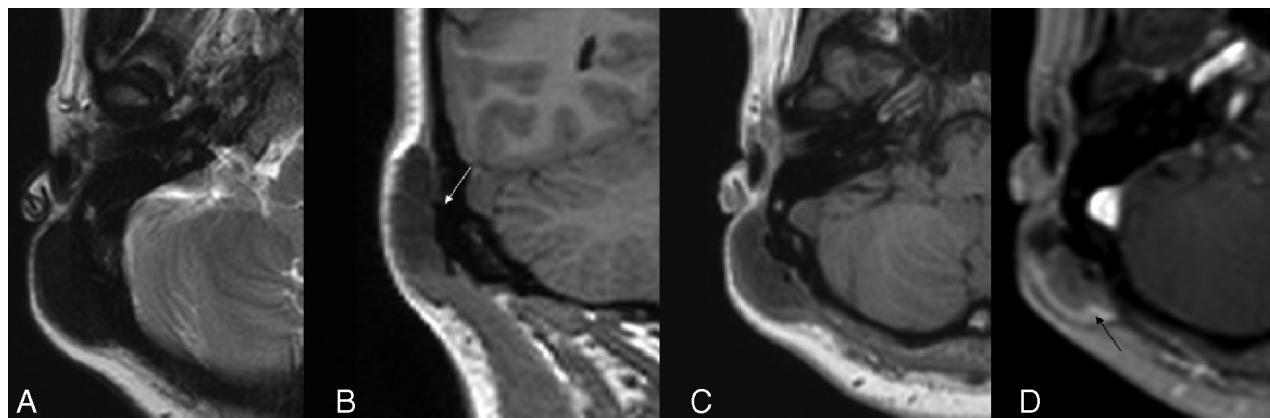


**FIG 3.** Case 1. MR images with and without contrast. Axial T2 (A), coronal and axial T1 (B and C), and postgadolinium axial (D) T1-weighted images show a T1- and T2-hypointense (to muscle), mildly enhancing broad-based, exophytic postauricular lesion emanating from the outer table of the right temporal bone (arrow in B). There is no signal change in the underlying bone and no intramedullary or intracranial extension. A thin, peripheral rim of enhancement is seen (arrow in D).

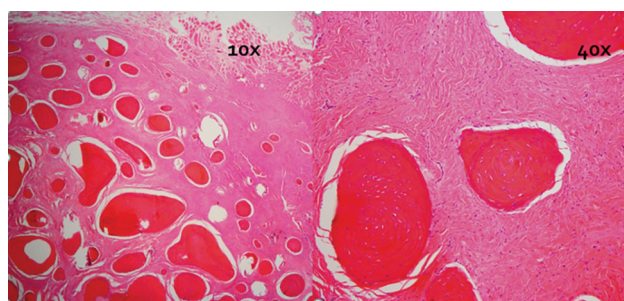


**FIG 4.** Case 1. Histology under low-power (10 $\times$ ) and high-power (40 $\times$ ) fields. Note numerous rounded ossified bodies composed of either woven or lamellar bone within a bland fibrous stroma. No atypia, mitotic activity or osteoblastic rimming are identified.



**FIG 5.** Case 2. On clinical examination, a 3  $\times$  2 cm left retroauricular bony protuberance over the mastoid area is noted.

ivory osteoma. With growth, that initial solidly calcified component appeared as a bony stalk with surrounding more irregular calcifications. A subsequent brain MR imaging with and without contrast demonstrated a predominantly T2-hypointense mass with

an enhancing rim (Fig 10). The leading differential diagnosis was an osteochondroma. Given the interval growth, the patient was referred to neurosurgery, and a PET/CT was acquired. The lesion was found to be FDG-avid (Fig 11).

The patient underwent a right temporal craniectomy with mesh cranioplasty and an excision of a 3.3 cm, tan-white, rubbery, fibro-osseous mass. On histologic analysis, the tumor was composed of spindle cells with fascicular architecture and entrapped islands of bone. Findings were most consistent with a Bullough lesion (Fig 12). Of note, occasional mitotic features were observed, a finding that differs from those in other reported cases of Bullough lesions. The patient did well postoperatively without any clinical or imaging findings or recurrence for 18 months.

### Literature Review

To date, 10 cases of PFOLT have been reported in the literature.<sup>1-7</sup> The cases have varied in age (10–70 years; mean, 37.5 years) and have been seen predominantly in females (female/male ratio, 7:3) and on the right side (right/left ratio, 8:2). All patients presented with a firm retroauricular mass that had been slowly enlarging for many years (range, 1–15 years), except for case 2 from the original case reports by Selesnick et al,<sup>1</sup> in which the patient discovered the mass 5 days before presentation. On examination, the lesion presented as a nontender, firm or hard, immobile, exophytic, retroauricular mass with smooth surfaces and without overlying skin or soft-tissue abnormalities. In only 1 pediatric case reported by Jiang et al<sup>5</sup> was the mass tender to touch. No lymphadenopathy was noted. The findings of the remainder of the regional and systemic physical examination were unremarkable. No comorbidities were reported in any of the cases, except in case 2 by Lee et al,<sup>4</sup> whose patient had a history of hepatitis B, and the pediatric case reported by Jiang et al with a family history of polycystic kidney disease. No history of preceding trauma had been reported before the appearance of the mass, except in case 2 by Lee et al, whose patient had a history of a fall in childhood with the appearance of a bean-sized lesion slowly growing for years in the same location as the subsequent

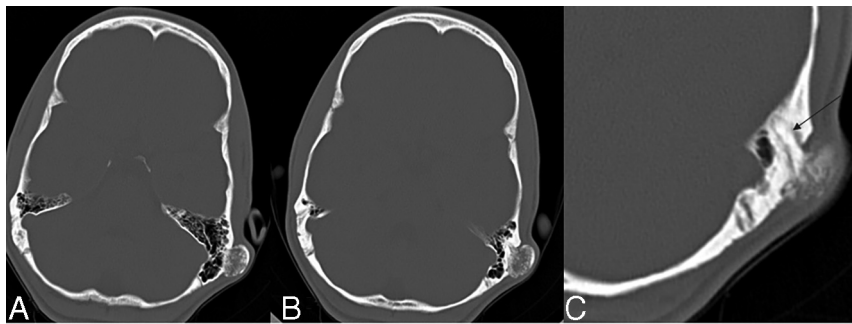


**FIG 6.** Case 2. Axial noncontrast CT images through the temporal bones (A and B) show a well-margined exophytic mass based along the lateral mastoid cortex with a densely calcified rim and a central heterogeneously calcified component. Magnified axial CT image (C) shows a densely calcified stalk (black arrow) that extends into the occipitomastoid suture.

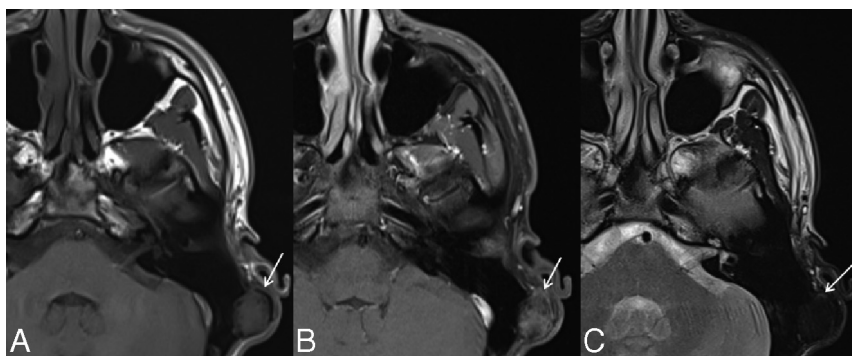


**FIG 7.** Case 2. MR images with and without contrast. Axial T1 (A), axial T1 postgadolinium fat-saturated (B), and axial T2-weighted (C) images show a thin peripheral signal void (arrow in A) and central intermediate signal intensity on noncontrast T1WI with mild heterogeneous enhancement (arrow in B) and diffusely low T2 signal intensity (arrow in C).

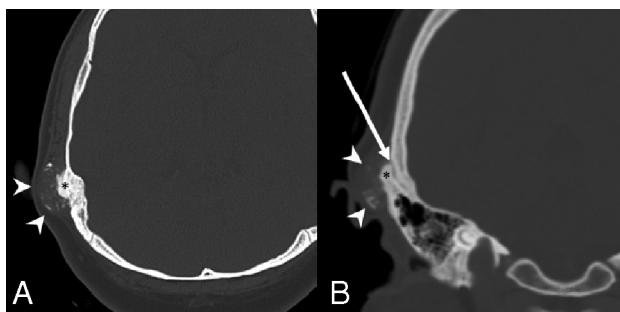


**FIG 8.** Case 3. Axial and coronal noncontrast CT images (A and B) demonstrate an irregularly calcified mass (white arrowheads) centered over the right temporal outer cortex at the level of the occipitomastoid suture (white arrow). Note the solidly calcified bony stalk (black asterisk). No gross destruction of the outer table cortex is seen, and there is no intraosseous or intracranial extension. The lesion uplifts the overlying scalp.

Bullough lesion. In the case described by Jiang et al, the mass was first noticed when the patient had a minor trauma.

Two patients underwent plain skull radiographs, which showed a wide-based retroauricular bony exostosis with a speckled appearance in 1 case and spiculated margins and a somewhat sunburst appearance in the other.<sup>2,5</sup> All the reported patients

underwent CT of the head without contrast. On imaging, the size of the mass ranged from 1.7 to 5.5 cm.<sup>4,6</sup> A well-defined, heterogeneous, broad-based, exophytic, retroauricular mass, emanating from the outer cortex of the temporal bone and in close relationship to the occipitomastoid suture was seen in all cases. The lesion consisted of varying degrees of mineralization, ranging from small punctate foci of calcification to coarse calcification, interposed within a more lucent ground-glass matrix. The underlying cortex was intact, without intramedullary or intracranial extension, but elevation of the overlying scalp soft tissue was reported in all cases. No involvement of the mastoid air cells was reported. Sia et al<sup>2</sup> also noticed an irregular contour of the underlying cortex in 1 case and some remodeling of the underlying cortex in another case, but with an intact bony cortex without intramedullary or intracranial extension in both cases. In 2 cases, a pedunculated attachment of the lesion to the underlying bone was reported.<sup>6,7</sup> None of these patients were evaluated by MR imaging.

In all cases, the lesion was surgically excised and sent for histologic examination. On microscopy, the lesion characteristically showed a mixture of ovoid-to-spherical bone islands of various sizes composed of either woven or lamellar bone and embedded in a dense fibrocollagenous stroma. Direct continuity between collagen from bone and the surrounding fibrous stroma has been identified.<sup>2,6</sup> Immunohistochemical stains for CD34, desmin, S-100 protein, smooth-muscle actin, epithelial membrane antigen, carcinoembryonic antigen, progesterone receptor, signal transducer and activator of transcription 6, and pancytokeratin were negative, with a negligible Ki-67 proliferation index.<sup>2,4</sup>  $\beta$ -catenin staining did not show nuclear localization, which would be suggestive of aberrant Wnt/ $\beta$ -catenin signaling, and only showed weak cytoplasmic positivity in the peripheral merging areas of osseous islands in 1 case.<sup>4</sup> In addition, mouse double minute 2 homolog was tested in 1 case and was not amplified, which would be seen in certain low-grade osteosarcomas. Overall, these results are consistent with a fibro-osseous lesion without muscle, nerve, vascular, or epithelial differentiation. No mitotic activity or cellular atypia has been reported. No evidence of guanine nucleotide stimulatory protein (GNAS) mutation, which is characteristically present in fibrous dysplasia, has been found.<sup>4</sup>

## DISCUSSION

This case series describes the clinical, pathologic, and radiologic features in 3 cases of PFOLT. Most existing publications on this

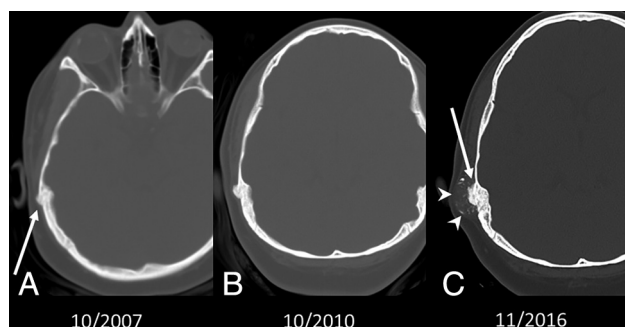


**FIG 9.** Case 3. Axial noncontrast CT images across time demonstrating the slow, interval growth of the retroauricular mass along the outer cortex of the right temporal bone. Also note that the lesion was initially a solidly calcified bony stalk, imaging similar to a peripheral ivory osteoma (white arrow in A). As the lesion grew, the ossification was less solid at the periphery and more irregular (white arrowheads in C) with persistence of the initial bony stalk (arrow in C).

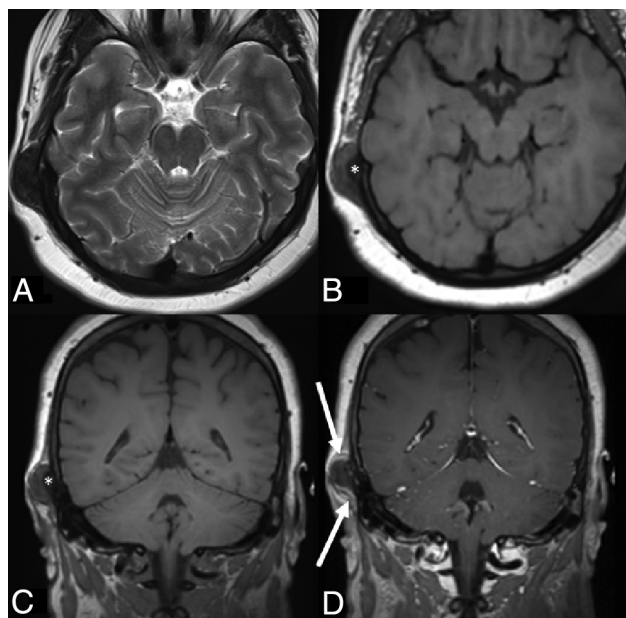


**FIG 10.** Case 3. MR images with and without contrast. Axial T2-weighted image (A) demonstrates the homogeneous T2-hypointense signal of the lesion. The lesion is predominantly T1-hypointense on the axial and coronal noncontrast T1-weighted images (B and C), particularly centrally, corresponding to the more densely calcified bony stalk (white asterisk). A largely peripheral cap of enhancement (white arrows) is noted on the coronal, postcontrast T1-weighted image.

topic have been in the pathology, otolaryngology, and neurosurgery literature. We believe this imaging-focused series is the first one in the radiology literature with multimodality imaging appearances, including plain film, CT, MR imaging, and PET. Given the distinctive imaging features, familiarity of radiologists with this entity may allow an earlier prospective diagnosis.

On CT, PFOLTs are well-margined, protuberant, calcified masses in the retroauricular region, emanating from the outer cortex near or from the occipitomastoid suture. The degree of calcification ranges from ground-glass (case 1) to more a heterogeneous

speckled appearance (cases 2 and 3). Stalk-like attachment to the outer cortex is intermittently identified. The lesion is distinct from the marrow with no marrow continuity with the parent bone. No abnormal osseous density in the adjacent medullary cavity is present. On MR imaging, the lesions are markedly hypointense on T2-weighted images with mild heterogeneous enhancement. There is no extension of this lesion into the overlying scalp or surrounding soft tissues. In 2 cases, peripheral rimlike enhancement was noted on MR imaging.

Case 3 demonstrated an interval increase in size and PET avidity. Also of note, occasional mitotic figures were observed in this case on histology. Although the lesion is considered benign, case 3 suggests a more aggressive variant.

The imaging differential diagnosis of PFOLT includes fibrous dysplasia (FD), ossifying fibroma, osteoma, osteochondroma, surface osteosarcoma, and periosteal chondrosarcoma.

FD is a fibro-osseous lesion with approximately 110 reported cases involving the temporal bone.<sup>4,8,9</sup> FD, unlike PFOLT, is usually nonprotuberant and shows growth during childhood but becomes static after puberty.<sup>5,10</sup> Protuberant variants of FD, so-called “fibrous dysplasia protuberans,” are extremely rare, and only a few cases of this entity have been reported.<sup>11,12</sup> FD is usually associated with a mutation in the *GNAS1* gene,<sup>13,14</sup> whereas this mutation has not been found in PFOLT,<sup>4</sup> suggesting a different molecular pathogenesis of PFOLT. On imaging, FD is a poorly defined, nonprotuberant, intraosseous- or intramedullary-based lesion with bone expansion and disruption of the bony architecture with a ground-glass matrix. Histologically, FD contains curvilinear trabeculae of woven or occasionally lamellar bone, with inconspicuous osteoblastic rimming embedded within bland fibrous stroma. Ossifying fibroma is also an intramedullary-based, expansile, ground-glass lesion but is more localized, round or ovoid, with thin sharply circumscribed borders.<sup>15</sup> Only a handful of cases of ossifying fibroma have been described in the temporal bone.<sup>16,17</sup>

Osteoma is a benign osteoblastic tumor composed of well-differentiated mature osseous tissue resembling dense cortical bone, though cancellous bone may be seen.<sup>18</sup> The most common sites are the frontal and ethmoid sinuses; however, in the temporal bone, the external auditory canal is the most common site of origin, followed by the mastoid and squamous portion.<sup>18</sup> Histologically, it shows an admixture of lamellar and woven bone with Haversian-like canals, while a minority are composed of trabecular bone. Only a few cases of mastoid osteoma have been reported, and these can be pedunculated or sessile well-demarcated hyperdense masses arising from the lateral mastoid cortex without a predilection for the occipitomastoid suture.<sup>19-24</sup>

Osteochondroma is the most common benign tumor of bone but is uncommon in the head and neck.<sup>25</sup> On CT, the lesion is composed of cortical and medullary bone protruding from and continuous with the underlying bone with an overlying cartilage cap. There is pathognomonic cortical and marrow continuity of the lesion and the parent bone. MR imaging is the best radiologic technique for visualizing the effect of the lesion on surrounding structures and evaluating the hyaline cartilage cap.<sup>25</sup> Microscopically, these lesions contain an outer fibrous periosteal layer and a cartilage cap with underlying ossification, which is continuous with the cortex and marrow space.

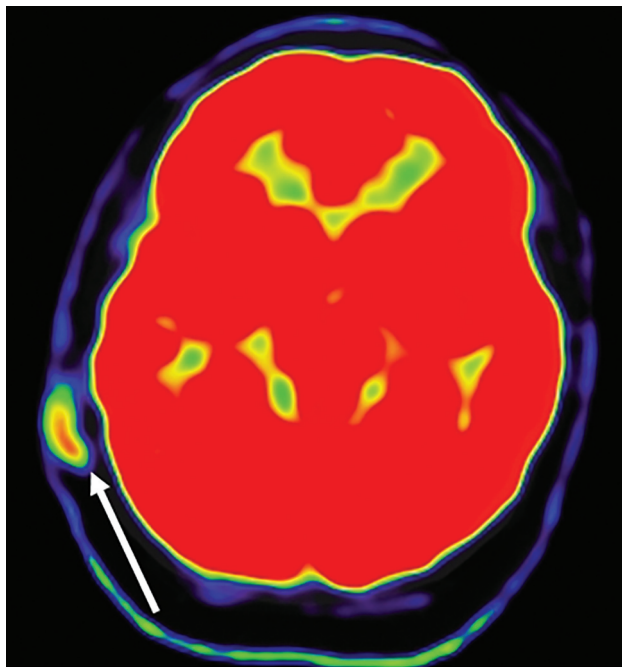


**FIG 11.** Case 3. FDG-PET image demonstrates FDG-avidity of the lesion (white arrow), consistent with the occasional mitotic features at histology.

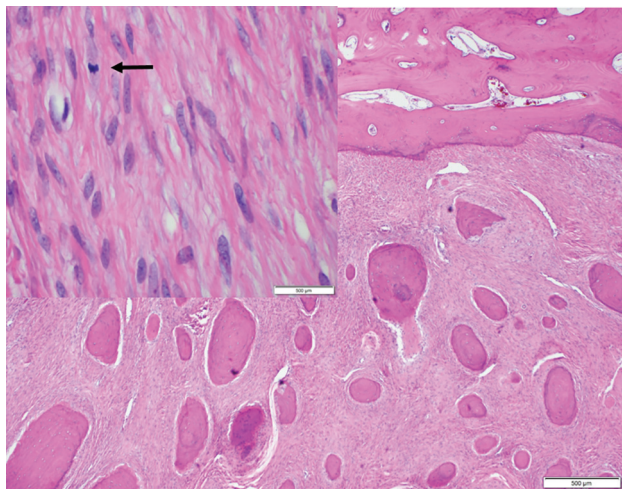


**FIG 12.** Case 3. Histology under a low-power field demonstrates numerous round ossified bodies within a proliferation of bland spindle cells. The fibrous stroma shows occasional mitotic figures (arrow in inset); however, no atypia is identified.

Osteosarcoma is a primary malignant bone tumor in which neoplastic cells produce osteoid. Surface osteosarcomas are rare variants of osteosarcoma that include parosteal osteosarcoma, periosteal osteosarcoma, and high-grade surface osteosarcoma.<sup>26,27</sup> The parosteal subtype, which was first referred to as “juxtacortical osteosarcoma,” is the most frequently encountered one. These tumors are rare in the temporal bone and have been identified in the mastoid segment and glenoid fossa.<sup>28</sup> On CT, they present as aggressive soft-tissue masses with calcification, cortical thickening, periosteal new bone formation, and invasion of the surrounding soft

tissue.<sup>29,30</sup> On MR imaging, the lesion is hyperintense on T2-weighted images with enhancement.<sup>29</sup> Histologically, these lesions demonstrate broad, woven bone trabeculae embedded in fibrous stroma and molecularly demonstrate CDK4a and use double minute 2 homolog amplification.<sup>31</sup>

Periosteal chondrosarcoma is a rare malignant cartilaginous tumor arising from the bony surfaces of the long bone and is extremely rare in craniofacial bones. On CT, the tumor is juxtacortical with thickening or erosion of the underlying cortex and contains calcific densities characteristic of cartilage tumors.<sup>32</sup> On MR imaging, the lesion is T2-hyperintense with enhancement of the periphery and septations. Low signal and punctate foci of mineralization can be seen on both T1- and T2-weighted sequences.<sup>32</sup> Histologically, these are atypical chondroid lesions with secondary calcification and ossification eroding the outer cortex, without invading the bone marrow.

As noted above, a PFOLT has distinct radiographic and histologic features that help differentiate it from these other lesions. This includes a relationship to the occipitomastoid suture, lack of continuity with the underlying medullary cavity, lack of a cartilage cap, lack of a periosteal reaction, and lack of T2-hyperintensity on MR imaging. Morphologically, a PFOLT shows a mixture of ovoid-to-spherical bone islands of various sizes composed of either woven or lamellar bone and embedded in a dense fibrocollagenous stroma.

## CONCLUSIONS

We have described the multimodality imaging appearance of a Bullough lesion in 3 cases, with distinct imaging features that can help suggest the correct diagnosis.

Disclosures: Gul Moonis—UNRELATED: Royalties: Wolters Kluwer, Comments: US \$140 in 2020.

## REFERENCES

- Selesnick SH, Desloge RB, Bullough PG. **Protuberant fibro-osseous lesions of the temporal bone: a unique clinicopathologic diagnosis.** *Am J Otol* 1999;20:394–96 [Medline](#)
- Sia SF, Davidson AS, Soper JR, et al. **Protuberant fibro-osseous lesion of the temporal bone: “Bullough lesion.”** *Am J Surg Pathol* 2010;34:1217–23 [CrossRef Medline](#)
- Nagarajan K, Jothiramingam SB. **3D CT appearance of exophytic mastoid fibro-osseous lesion.** *Indian J Otol* 2013;19:143 [CrossRef](#)
- Lee M, Song JS, Chun SM, et al. **Protuberant fibro-osseous lesions of the temporal bone: two additional case reports.** *Am J Surg Pathol* 2014;38:1510–05 [CrossRef Medline](#)
- Jiang B, Mushlin H, Zhang L, et al. **Bullough’s bump: unusual protuberant fibro-osseous tumor of the temporal bone: case report.** *J Neurosurg Pediatr* 2018;21:107–11 [CrossRef Medline](#)
- Sturdà C, Rapisarda A, Gessi M, et al. **Bullough’s lesion: an unexpected diagnosis after the resection of a slowly growing osseous-like retroauricular bump: case report and review of the literature.** *World Neurosurg* 2019;122:372–75 [CrossRef Medline](#)
- Maroun CA, Khalifeh I, Faddoul DS, et al. **A patient with a protuberant fibro-osseous lesion of the temporal bone.** *J Craniofac Surg* 2019;30:e453–54 [CrossRef Medline](#)
- Kim YH, Song JJ, Choi HG, et al. **Role of surgical management in temporal bone fibrous dysplasia.** *Acta Otolaryngol* 2009;129:1374–79 [CrossRef Medline](#)

9. Silu M, Gupta G. External auditory canal stenosis due to isolated fibrous dysplasia of temporal bone: a case report. *Int J Otorhinolaryngol Head Neck Surg* 2019;6:204 [CrossRef](#) [Medline](#)
10. Kushchayeva YS, Kushchayev SV, Glushko TY, et al. Fibrous dysplasia for radiologists: beyond ground glass bone matrix. *Insights Imaging* 2018;9:1035–56 [CrossRef](#) [Medline](#)
11. Dorfman HD, Ishida T, Tsuneyoshi M. Exophytic variant of fibrous dysplasia (fibrous dysplasia protuberans). *Hum Pathol* 1994;25:1234–37 [CrossRef](#) [Medline](#)
12. Hamadani M, Awab A, Rashid A, et al. Fibrous dysplasia protuberans in a patient with McCune-Albright syndrome. *J Coll Physicians Surg Pak* 2006;16:376–77 [Medline](#)
13. Weinstein LS, Shenker A, Gejman PV, et al. Activating mutations of the stimulatory G protein in the McCune-Albright syndrome. *N Engl J Med* 1991;325:1688–95 [CrossRef](#) [Medline](#)
14. Lee SE, Lee EH, Park H, et al. The diagnostic utility of the GNAS mutation in patients with fibrous dysplasia: meta-analysis of 168 sporadic cases. *Hum Pathol* 2012;43:1234–42 [CrossRef](#) [Medline](#)
15. Khoury NJ, Naffaa LN, Shabb NS, et al. Juvenile ossifying fibroma: CT and MR findings. *Eur Radiol* 2002;12(Suppl 3):S109–13 [CrossRef](#) [Medline](#)
16. Levine PA, Wiggins R, Archibald RW, et al. Ossifying fibroma of the head and neck: involvement of the temporal bone- and unusual and challenging site. *Laryngoscope* 1981;91:720–25 [CrossRef](#) [Medline](#)
17. Vlachou S, Terzakis G, Doundoulakis G, et al. Ossifying fibroma of the temporal bone. *J Laryngol Otol* 2001;115:654–56 [CrossRef](#) [Medline](#)
18. Jeong J, Choi YJ, Hong CE, et al. Giant osteoma in the mastoid of the temporal bone: complete excision of a rare tumor. *Otol Neurotol* 2018;39:e894–96 [CrossRef](#) [Medline](#)
19. Singh RK, Goyal A, Kumar A, et al. Mastoid osteoma of temporal bone: a rare case report. *J Clin Diagn Res* 2017;11:MD01–2 [CrossRef](#) [Medline](#)
20. Kandakure VT, Lahane VJ, Mishra S. Osteoma of mastoid bone; a rare presentation—case report. *Indian J Otolaryngol Head Neck Surg* 2019;71:1030–32 [CrossRef](#) [Medline](#)
21. Park SJ, Kim YH. A case of giant osteoma developed from the mastoid cortical bone. *Korean J Audiol* 2012;16:95–98 [CrossRef](#) [Medline](#)
22. Cheng J, Garcia R, Smouha E. Mastoid osteoma: a case report and review of the literature. *Ear Nose Throat J* 2013;92:E7–9 [Medline](#)
23. Viswanatha B. Characteristics of osteoma of the temporal bone in young adolescents. *Ear Nose Throat J* 2011;90:72–79 [CrossRef](#) [Medline](#)
24. Lee RE, Balkany TJ. Giant mastoid osteoma with postoperative high-frequency sensorineural hearing loss. *Ear Nose Throat J* 2008;87:23–25 [CrossRef](#) [Medline](#)
25. Murphey MD, Choi JJ, Kransdorf MJ, et al. Imaging of osteochondroma: variants and complications with radiologic-pathologic correlation. *Radiographics* 2000;20:1407–34 [CrossRef](#) [Medline](#)
26. Nouri H, Ben Maitigue M, Abid L, et al. Surface osteosarcoma: clinical features and therapeutic implications. *J Bone Oncol* 2015;4:115–23 [CrossRef](#) [Medline](#)
27. Raymond AK. Surface osteosarcoma. *Clin Orthop Relat Res* 1991;140–48 [Medline](#)
28. Tan JH, Miyakoshi A, Mafee MF. Imaging of fibro-osseous lesions of the temporal bone. *Oper Tech Otolaryngol Head Neck Surg* 2014;25:96–109 [CrossRef](#)
29. Murphey MD, Jelinek JS, Temple HT, et al. Imaging of periosteal osteosarcoma: radiologic-pathologic comparison. *Radiology* 2004;233:129–38 [CrossRef](#) [Medline](#)
30. Villemure-Poliquin N, Trudel M, Labonté S, et al. Low-grade surface osteosarcoma of the temporal bone in paediatric patients: a case report and literature review. *Clin Med Insights Pediatr* 2019;13:1179556519855381 [CrossRef](#) [Medline](#)
31. Yoshida A, Ushiku T, Motoi T, et al. Immunohistochemical analysis of MDM2 and CDK4 distinguishes low-grade osteosarcoma from benign mimics. *Mod Pathol* 2010;23:1279–88 [CrossRef](#) [Medline](#)
32. Chaabane S, Bouaziz MC, Drissi C, et al. Periosteal chondrosarcoma. *AJR Am J Roentgenol* 2009;192:W1–6 [CrossRef](#) [Medline](#)